MEDICAL SCIENCE MONITOR

LAB/IN VITRO RESEARCH

e-ISSN 1643-3750
© Med Sci Monit, 2019; 25: 1242-1253
DOI: 10.12659/MSM.912421

Received: 2018.07.31
Accepted: 2018.09.14
Published: 2019.02.15

Long Non-Coding RNA TFAP2A-AS1 Inhibits Cell Proliferation and Invasion in Breast Cancer via miR-933/SMAD2

Authors' Contribution:
Study Design A
Data Collection B
Statistical Analysis C
Data Interpretation D
Manuscript Preparation E
Literature Search F
Funds Collection G

ABCD 1 Bin Zhou
EFG 2 Haiyan Guo
ABCDEFG 3 Jinhai Tang

1 Department of General Surgery, Jiangsu Cancer Hospital (Affiliated Cancer Hospital of Nanjing Medical University), Nanjing, Jiangsu, P.R. China
2 Department of Infectious Diseases, Jiangsu Province Hospital of Traditional Chinese medicine (TCM), Affiliated Hospital of Nanjing University of TCM, Nanjing, Jiangsu, P.R.China
3 Department of General Surgery, First Affiliated Hospital of Nanjing Medical University, Nanjing, Jiangsu, P.R. China

* Bin Zhou and Haiyan Guo are co-first authors

Corresponding Author: Jinhai Tang, e-mail: tjh7896@aliyun.com

Source of support: This work was supported by the National Key Research and Development Program of China (No. 2016YFC0905900); the "333" Talent Project of Jiangsu Province [No. 4(2016)]; the National Key Clinical Specialist Construction Programs of China [No. 544 (2013)]; and the Natural Science Foundation of Jiangsu Province (No. BK20151579)

Background: It is well documented that long non-coding RNAs (lncRNAs) are involved in the progression of multiple human tumors by sponging microRNAs (miRNAs). However, whether lncRNA TFAP2A-AS1 plays a role in the tumorigenesis of breast cancer (BC) remains undetermined.

Material/Methods: Real-time PCR (qRT-PCR) assay was performed to detect the relative mRNA expression of TFAP2A-AS1 and miR-933. Flow cytometry analysis, CCK-8 assay, and Transwell assay were applied to detect the effects of TFAP2A-AS1 overexpression on cell cycle, apoptosis, viability, and invasion of BC cells. *In vivo* proliferation assay was performed to evaluate the effects of TFAP2A-AS1 overexpression on tumor growth. Bioinformatics methods, dual-luciferase reporter, RNA immunoprecipitation (RIP), and RNA pull-down assays were used to predict and validate the interaction between TFAP2A-AS1 and miR-933, as well as SMAD2 and miR-933. Western blot assay was performed to examine the protein expression of SMAD2 in treated BC cells.

Results: TFAP2A-AS1 expression was significantly lower in BC tissues and cell lines, and patients with high TFAP2A-AS1 expression exhibited a better prognosis than those with low TFAP2A-AS1 expression. Overexpression of TFAP2A-AS1 in BC cells caused cell cycle arrest, promoted cell apoptosis, suppressed cell ability, and attenuated cell invasion *in vitro*, and inhibited tumor growth *in vivo*. TFAP2A-AS1 was revealed to act as a miRNA sponge for miR-933 and then regulated the expression of Smad2.

Conclusions: Results from the present study suggest that TFAP2A-AS1 acts as a tumor suppressor in BC via the miR-933/SMAD2 axis.

MeSH Keywords: Breast Neoplasms • MicroRNAs • RNA, Long Noncoding • Smad2 Protein

Full-text PDF: https://www.medscimonit.com/abstract/index/idArt/912421

Indexed in: [Current Contents/Clinical Medicine] [SCI Expanded] [ISI Alerting System] [ISI Journals Master List] [Index Medicus/MEDLINE] [EMBASE/Excerpta Medica] [Chemical Abstracts/CAS]

Background

Breast cancer (BC), derived from breast tissues, is one of the most common type of cancers in women [1,2]. BC can occur at any age, but it tends to develop more readily in older individuals [3]. Although the causes of BC are not fully understood, multiple risk factors of BC have been identified, including lack of physical exercise, alcohol intake, obesity, and being female [4,5]. Because of the development of early-stage cancer diagnosis technologies, BC screening has significantly reduced the mortality rate of BC; however, BC still ranks as the second leading cause of cancer-related death worldwide [6]. The conventional treatment for BC is surgical resection followed by chemotherapy, but this can cause damage aesthetic appearance, and the reoccurrence rate remains high [7]. Elucidating the mechanisms of tumorigenesis of BC not only could contribute to understand this disease, but could also help develop new effective therapeutic targets for BC patients.

Long non-coding RNAs (lcnRNAs), characterized by a length of more than 200 nucleotides, and microRNAs (miRNAs), characterized by length less than 22 nucleotides, are the 2 most important non-coding RNAs (ncRNAs), which lack protein-encoding capacity [8]. Previous studies have demonstrated that lncNRAs and miRANs participate in multiple physiological processes, such as cell proliferation, tissue differentiation, and metabolic regulation [8,9]. Dysregulation of lncRNAs and miRNAs can cause a series of dysfunctions and diseases, including various human cancers [9]. Recently, emerging evidence has suggested a cross-modulation between lncRNAs and miRNAs [10,11]. lncRNAs may serve as competing endogenous RNA (ceRNA) or an RNA sponge in regulating the expression and functions of miRNAs [12–14]. miRNAs were also reported to be involved in gene expression regulation via binding to the 3'-untranslated regions (3'-UTR) of targeted genes [15]. The interaction of lncRNAs and miRNAs can affect the initiation and progression of multiple cancers by directly or indirectly regulating the expression of cancer-related genes [16]. TFAP2A-AS1 is a novel lncRNA with unclear functions located at chromosome 6q24.3. To the best of our knowledge, the expression and functions of TFAP2A-AS1 in breast cancer pathology have not yet been studied.

In the present study, we explored the functions and mechanisms of TFAP2A-AS1 in BC. TFAP2A-AS1 expression was first examined in BC tissues and cell lines, and gain-of-function assays were performed to evaluated the TFAP2A-AS1 effects on tumor growth *in vitro* and *in vivo*. To explore the possible mechanisms involved, bioinformatics analysis was performed to predict the targeted miRNA of TFAP2A-AS1. TFAP2A-AS1 was identified as a miRNA sponge for miR-933, which targeted the 3'-UTR of SMAD2. Our study revealed that lncRNA TFAP2A-AS1 can act as a tumor suppressor in BC by sponging miR-933 to release SMAD2.

Material and Methods

Clinical patient samples and cell culture

Thirty pairs of tumor tissues and adjacent normal tissues of BC patients were collected from the Jiangsu Cancer Hospital during the period 2013–2018. Written informed consent was obtained by every patient, and methods used were approved by the Ethics Committee of Jiangsu Cancer Hospital. The normal human mammary epithelial cell line MCF-10A and BC cell lines MCF-7, MDA-MB-231, MDA-MB-435, T47D, and SKBR-3 were all obtained from the Chinese Academy of Sciences (Shanghai, China). All cell lines were maintained at 37°C with 5% CO_2 and 95% O_2 in DMEM (Invitrogen, Carlsbad, CA, USA) supplemented with 10% fetal bovine serum (Sigma, USA), and penicillin (100 U/ml)/streptomycin (100 g/ml).

Cell transfection

TFAP2A-AS1 and its negative control, as well as miR-933 mimics/inhibitor and their negative control miR-NC/anti-NC, were used in the present study were all designed and obtained from GenePharma (Shanghai, China). In the *in vitro* cell transfection, BC cells were transfected with corresponding RNA molecules by using Lipofectamine 3000 (Invitrogen) according to the manufacturer's instructions. In the *in vivo* experiments, TFAP2A-AS1 cDNA was sub-cloned into the LV5 lentiviruses (GenePharma) and then MCF-7 cells were infected with the recombinant lentiviruses.

RNA extraction and quantitative real-time PCR (qRT-PCR) assay

Total RNAs from treated BC cell lines and tissues were all prepared using TRIzol reagent (Takara, Japan), and the cDNA was produced by 50 ng total RNAs using a BestarTM qPCR RT kit (DBI Bioscience, China). The amplification was performed on the ABI PRISM 7500 Sequence Detection System (Life Technologies, USA) with the BestarTM qPCR MasterMix (DBI Bioscience) according to the instructions obtained from the manufacturers. All primers used in the present study were synthesized by Sangon (Shanghai, China), and the sequence of primers were: GAPDH: F, 5'-TGT TCG TCA TGG GTG TGA AC-3', R, 5'-ATG GCA TGG ACT GTG GTC AT-3'; U1: F, 5'- GGG AGA TAC CAT GAT CAC GAA GGT', R, 5'-CCA CAA ATT ATG CAG TCG AGT TTC CC-3'; miR-933: F, 5'-ATT ATA TGT GCG CAG GGA GAC C-3', R, 5'-GCG AGC ACA GAA TTA ATA CGA CTC ACT ATA GG-3'; TFAP2A-AS1: F, 5'-CTT GAC AGC TCC AGG GGT TA-3', R, 5'-TCT AGA CTT GCA GGC ACA CA-3'; CDK6 F, 5'-GGC CTC AGC AGC CGC CTT AAG CTG A-3', R, 5'-CAG GAA AGA GTT TCT GAC AAA TT-3'; cyclin D1 F, 5'-GCT GCG AAG TGG AAA CCA TC-3', R, 5'-CCT CCT TCT GCA CAC ATT TGA A-3'; cyclin E1 F, 5'-GCC GCA GTA TCC CCA GCA AA-3', R, 5'-TCG CAC CAC TGA TAC CCT GA-3'.

Indexed in: [Current Contents/Clinical Medicine] [SCI Expanded] [ISI Alerting System] [ISI Journals Master List] [Index Medicus/MEDLINE] [EMBASE/Excerpta Medica] [Chemical Abstracts/CAS]

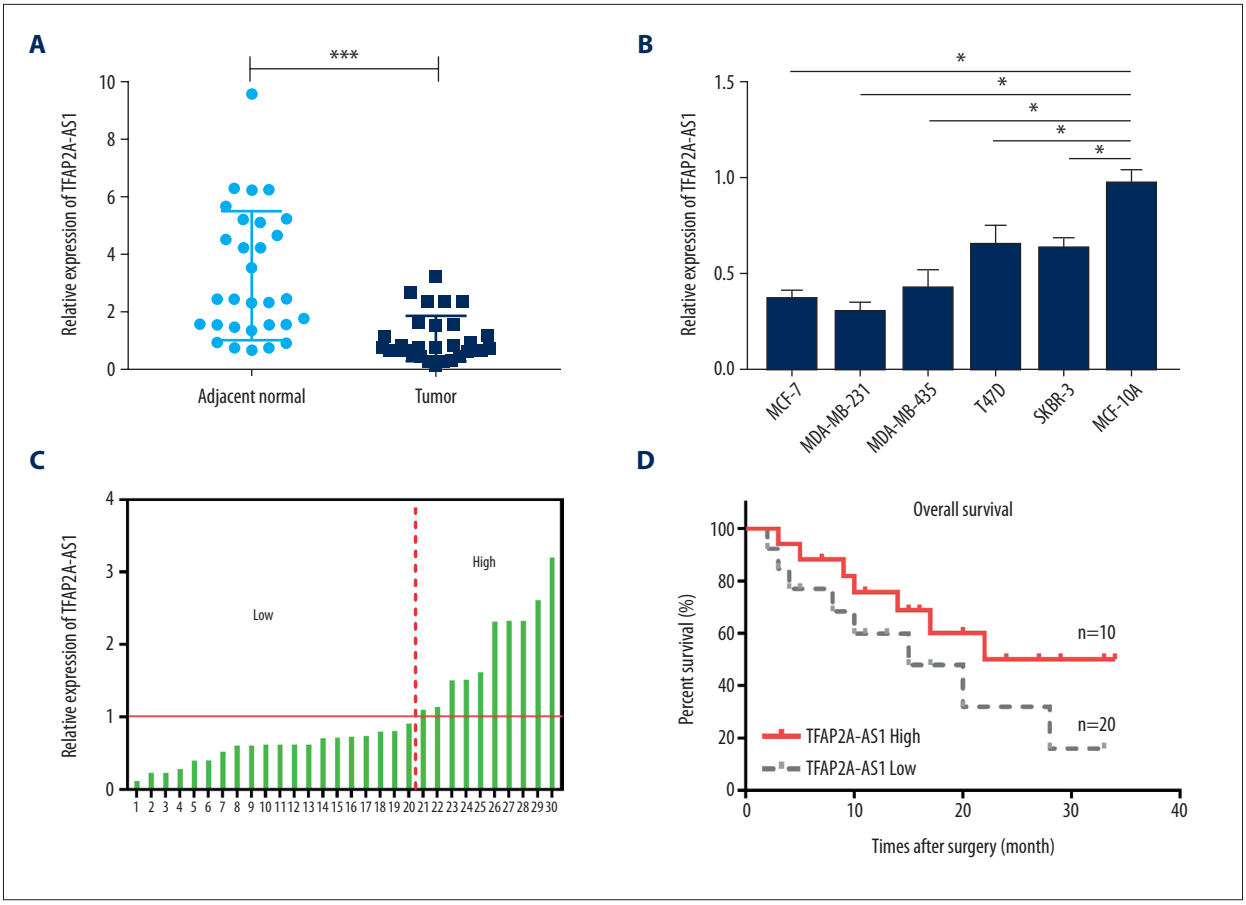

Figure 1. Expression of TFAP2A-AS1 in BC tissues and cell lines. (**A**) The relative mRNA expression of TFAP2A-AS1 in 30 pairs of BC tissues and adjacent normal tissues was assessed by qRT-PCR. (**B**) The relative mRNA expression of TFAP2A-AS1 in 5 BC cell lines (MCF-7, MDA-MB-231, MDA-MB-435, T47D, and SKBR-3) and the human mammary epithelial cell line MCF-10A, was evaluated by qRT-PCR. (**C, D**) Patients with low TFAP2A-AS1 expression (n=10) exhibited a worse prognosis than patients with high TFAP2A-AS1 expression (n=20).

Subcellular fractionation

To determine the cellular distribution of TFAP2A-AS1 in BC cells, the nuclear fraction of MCF-7 was isolated from cytoplasm using the PARIS kit (Life Technologies, USA) following the manufacturer's protocols. RNA was isolated from the nuclei and cytoplasm of MCF-7 cells, and the TFAP2A-AS1 expression in the nuclear and cytoplasm was measured by qRT-PCR. GAPDH and U1 were used as the cytoplasmic and nuclear controls, respectively.

Cell apoptosis and cycle analysis

Cell cycle and apoptosis of treated MCF-7 and MDA-MB-231 cells were evaluated using flow cytometry analysis. Briefly, 48 h after the TFAP2A-AS1 transfection, BC cells were collected and resuspended in DMEM at a concentration of 1×10^5 cells/well. Subsequently, the treated BC cells were fixed in ethanol for 30 min, and Annexin V-FITC and propidium iodide were used to stain cells for 15 min at room temperature. Finally, cell cycle and apoptosis were assessed using a flow cytometer (FACSCanto™ II, BD Biosciences).

Cell viability analysis

Cell viability of TFAP2A-AS1 transfected MCF-7 and MDA-MB-231 cells were evaluated using a Cell Counting kit-8 (CCK-8, Sigma, USA) according to the protocols provided by the manufacturer. In brief, MCF-7 and MDA-MB-231 cells were seeded into 96-well plates and incubated with TFAP2A-AS1 for 5 days. Optical density was detected using a microtiter plate reader (SpectraMax, Molecular Devices, USA) at 0, 1, 2, 3, 4, and 5 days.

Cell invasion analysis

Effects of TFAP2A-AS1 overexpression on the invasive ability of BC cells were evaluated by Transwell assay using the specific chamber (8-μm, Corning Incorporated, USA), coated with

Indexed in: [Current Contents/Clinical Medicine] [SCI Expanded] [ISI Alerting System] [ISI Journals Master List] [Index Medicus/MEDLINE] [EMBASE/Excerpta Medica] [Chemical Abstracts/CAS]

Table 1. Correlations between long non-coding RNA TFAP2A-AS1 expression and clinicopathologic characteristics in breast cancer.

Clinicopathologic characteristics	No. of patients	Long non-coding RNA TFAP2A-AS1		*P* value
		High	Low	
Age (year)				
>50	21	10 (47.6%)	11 (52.4%)	0.500
≤50	9	5 (55.6%)	4 (44.4%)	
Tumor size (cm)				
<3	19	12 (63.2%)	7 (36.8%)	0.287
≥3	11	5 (45.5%)	6 (54.5%)	
Differentiation grade				
Well/moderately	17	12 (70.6%)	5 (29.4%)	0.035*
Poorly/undifferentiated	13	4 (30.8%)	9 (69.2%)	
TNM stage				
0 & I & II	24	19 (79.2%)	5 (20.8%)	0.049*
III & IV	6	2 (33.3%)	4 (66.7%)	

* $P<0.05$, TNM stage – pathologic tumor, node, metastasis stage.

Matrigel matrix (BD Biosciences, Franklin Lakes, NJ, USA). Briefly, 500 µl of serum-free DMEM containing TFAP2A-AS1 overexpressed MCF-7 and MDA-MB-231 cells were added into the upper chamber. DMEM containing 10% FBS was added into the lower chamber. After incubation for 48 h, the invasive BC cells were fixed and stained using 0.5% crystal violet, and the number of invasive cells was counted using ImageJ software.

In vivo proliferation assay

Five-week-old male BALB/c nude mice were used in this study, and the animal experiments were approved by the Institutional Animal Care and Use Committee of Jiangsu Cancer Hospital. MCF-7 cells (1×10^6 cells/ml) transfected with LV-5/TFAP2A-AS1 recombinant lentiviruses were injected into the left flank of the nude mice. The tumor volume was measured every 3 days until 21 days, then the mice were sacrificed and the tumor weight was calculated.

Plasmid construction and dual-luciferase activity assay

For plasmid construction, the wild-type TFAP2A-AS1 and SMAD2 3'-UTR containing the miR-933 binding sites were inserted into the luciferase vector psi-CHECK2 (Promega, Madison, USA), named as psiCHECK2-TFAP2A-AS1-WT and SMAD2-WT, respectively. The TFAP2A-AS1 and SMAD2 3'-UTR containing the mutant miR-933 binding site were also sub-cloned into psi-CHECK2 to form psiCHECK2-TFAP2A-AS1-Mut and SMAD2-Mut, respectively.

The interaction between TFAP2A-AS1 and miR-933, as well as SMAD2 and miR-933, were assessed using dual-luciferase reporter assay system following the protocols obtained from the manufacturers. Renilla luciferase activity was normalized to Firefly luciferase activity.

Validation of TFAP2A-AS1 and miR-933 interaction

The interaction between TFAP2A-AS1 and miR-933 was verified by RNA immunoprecipitation (RIP) assay and RNA pull-down assay. For RIP assay, MCF-7 cells were collected and lysed with RIP lysis buffer, and then 50 µl of MCF-7 cell lysate was incubated with magnetic beads conjugated with a human anti-Argonaute2 (Ago2) antibody or negative control IgG in RIP buffer. Subsequently, proteinase K was used to digest proteins to RNAs were purified and validated by qRT-PCR. For RNA pull-down assay, miR-933 was transcribed with biotin-labeled RNA Mix using T7 RNA polymerase to form biotin-labeled miR-933, and RNeasy Mini Kit was used to purify targeted miR-933. After conjugation with streptavidin agarose beads, it was incubated with MCF-7 cell lysate for 2 h at room temperature. Finally, the beads were extracted using TRIzol reagent and qRT-PCR was used to analyze the enrichment.

Western blot assay

Total proteins of treated MCF-7 cells were prepared using RIPA buffer containing 1 mM PMSF. After centrifuging at 12 000 g for 15 min at 4°C, the supernatants were collected, and the protein concentration was determined via the BCA kit (Pierce, Rockford). Total proteins were then separated by 10% SDS-PAGE and

Indexed in: [Current Contents/Clinical Medicine] [SCI Expanded] [ISI Alerting System] [ISI Journals Master List] [Index Medicus/MEDLINE] [EMBASE/Excerpta Medica] [Chemical Abstracts/CAS]

transferred onto nitrocellulose membranes (Millipore, Billerica, MA, USA). Non-specific binding sites were blocked in the 5% low-fat dried milk for 2 h. After washing 3 times in TBST, the membranes were incubated overnight at 4°C with the primary antibodies against SMAD2 (Rabbit, 1: 500, ab53100, Abcam) and GAPDH (Rabbit, 1: 2500, ab9485, Abcam). Subsequently, the membranes were incubated with horseradish peroxidase-conjugated donkey-anti-rabbit secondary antibodies at room temperature for 2 h. Finally, the signals were detected with enhanced chemiluminescent reagents.

Statistical analysis

Data are all presented as mean ±SEM. The t test was used to compare difference between 2 groups, and one-way ANOVA was carried out to compare difference between more than 2 groups. GraphPad software (Ver. Prism 7, GraphPad Prism Software, La Jolla, CA, USA) was used to conduct the statistical analysis, and $P<0.05$ was considered as significant.

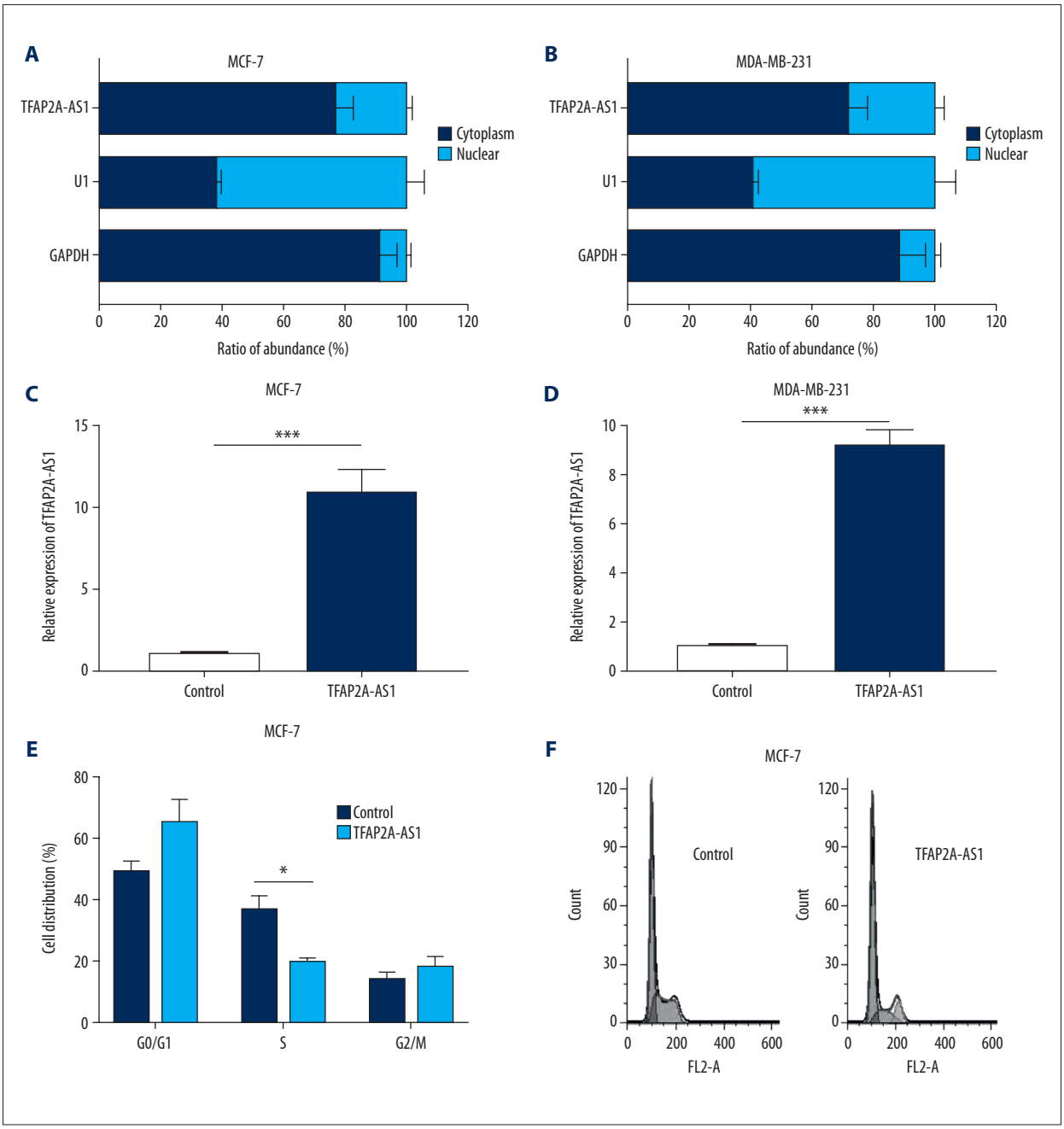

Indexed in: [Current Contents/Clinical Medicine] [SCI Expanded] [ISI Alerting System] [ISI Journals Master List] [Index Medicus/MEDLINE] [EMBASE/Excerpta Medica] [Chemical Abstracts/CAS]

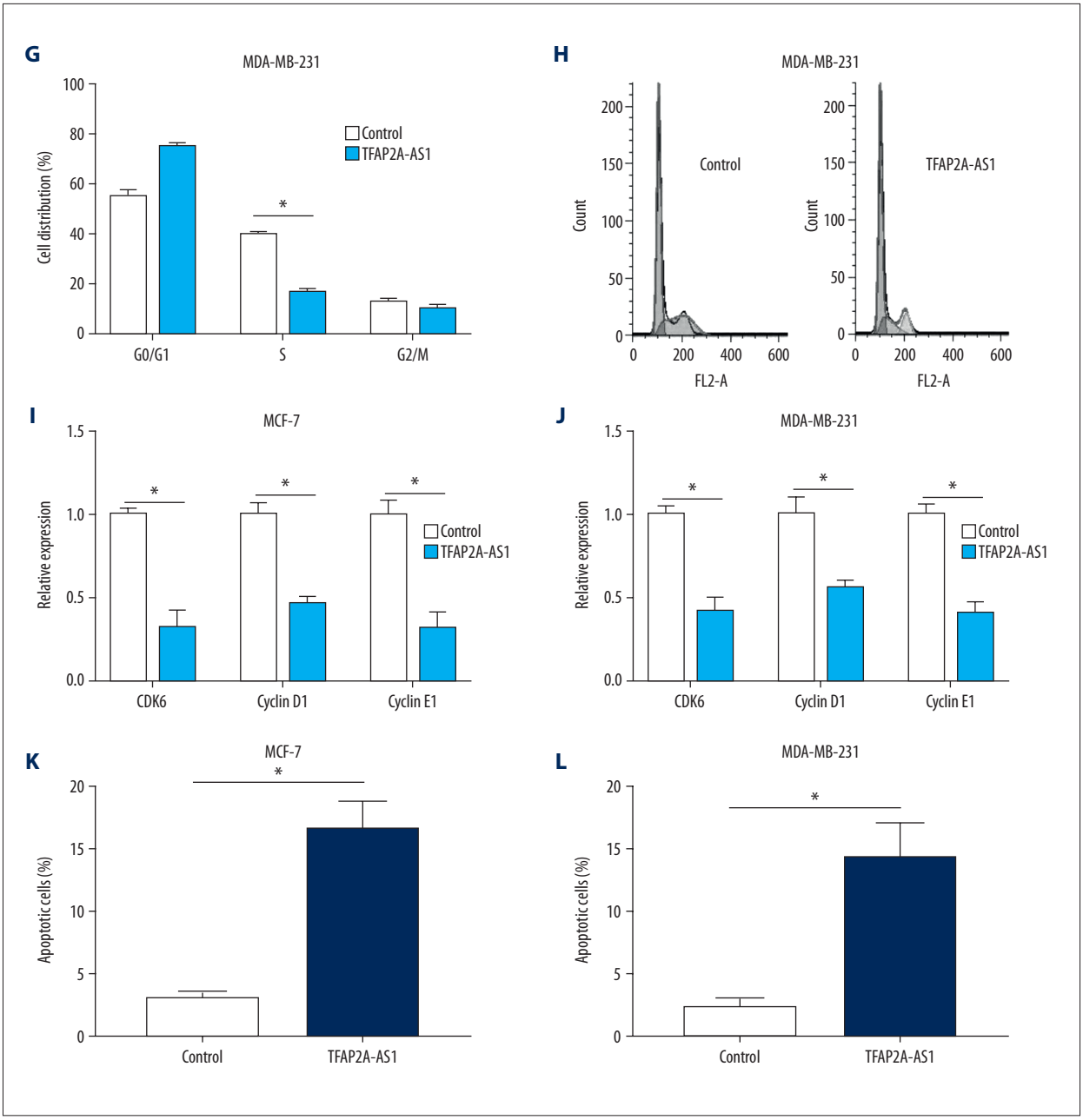

Figure 2. Effects of TFAP2A-AS1 overexpression on cell cycle and apoptosis of BC cell lines. (**A, B**) The cellular location of TFAP2A-AS1 in MCF-7 and MDA-MB-231 cells; the nucleus-retained U1 and cytoplasmic GAPDH was used as control. (**C, D**) Expression of TFAP2A-AS1 in MCF-7 and MDA-MB-231 cells transfected with TFAP2A-AS1 and its negative control were assessed by qRT-PCR. (**E–H**) Flow cytometry analysis was performed to analyze the cell cycle of MCF-7 and MDA-MB-231 cells transfected with TFAP2A-AS1. (**I, J**) The relative expression of CDK6, cyclin D1, and cyclin E1 in TFAP2A-AS1-overexpressed MCF-7 and MDA-MB-231 cells were measured by qRT-PCR. (**K, L**) Cell apoptosis of MCF-7 and MDA-MB-231 cells transfected with TFAP2A-AS1 and its negative control were evaluated by flow cytometry.

Indexed in: [Current Contents/Clinical Medicine] [SCI Expanded] [ISI Alerting System] [ISI Journals Master List] [Index Medicus/MEDLINE] [EMBASE/Excerpta Medica] [Chemical Abstracts/CAS]

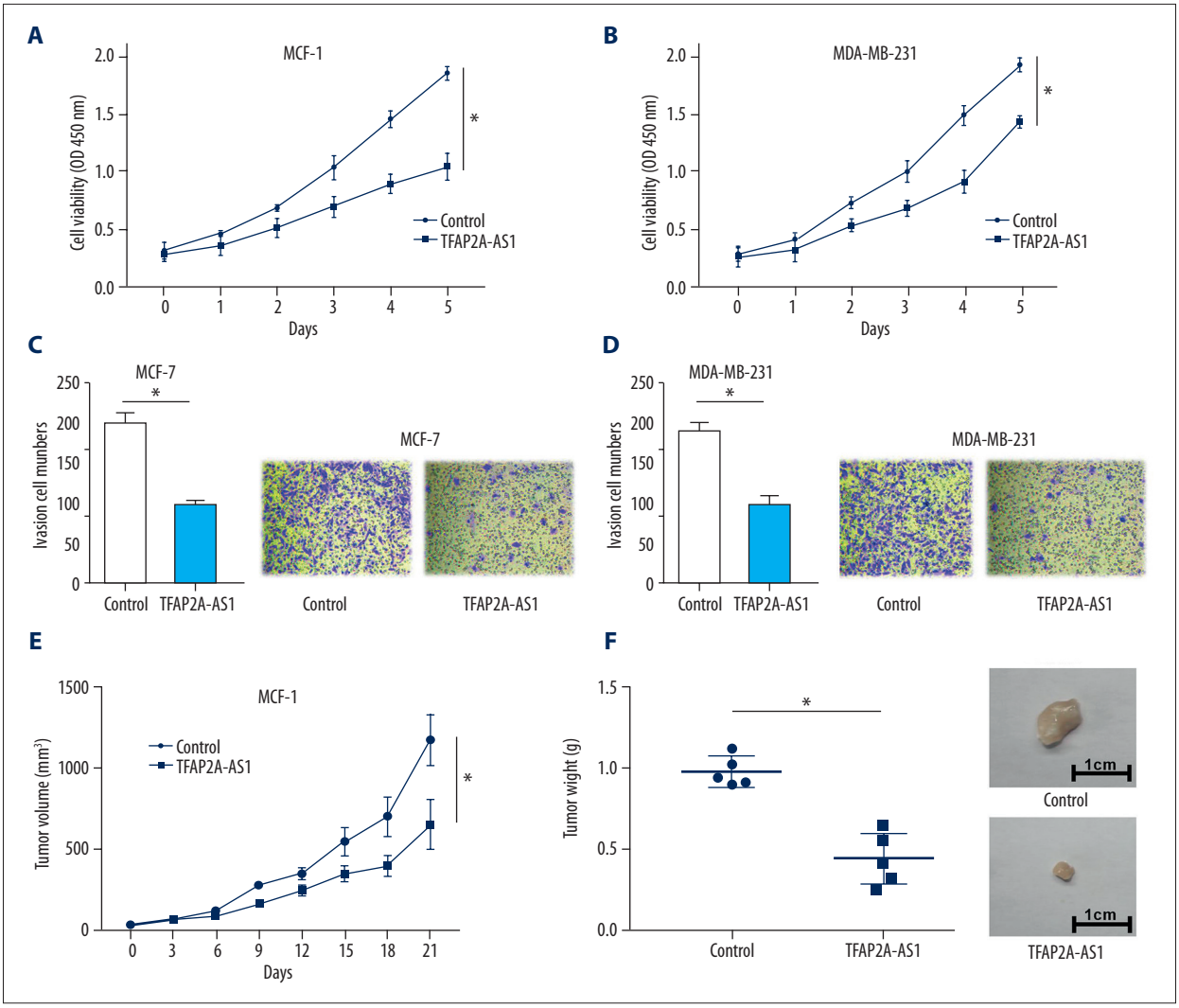

Figure 3. Effects of TFAP2A-AS1 overexpression on *in vitro* cell viability, invasion, and *in vivo* tumor growth. (**A, B**) Cell viability of TFAP2-AS1 overexpressed MCF-7 and MDA-MB-231 cells were examined by CCK-8 assay. (**C, D**) Cell invasion of TFAP2-AS1-overexpressed MCF-7 and MDA-MB-231 cells were assessed by Transwell assay. (**E, F**) An *in vivo* subcutaneous tumor model of TFAP2A-AS1-overexpressed MCF-7 cells was established, and the tumor volume and weight were measured.

Results

TFAP2A-AS1 expression was significantly downregulated in BC.

To investigate the role of TFAP2A-AS1 in the pathogenesis of BC, we first examined the relative mRNA expression of TFAP2A-AS1 by qRT-PCR in BC tissues and cell lines. Results showed that TFAP2A-AS1 expression was significantly decreased in BC tissues compared with adjacent normal tissues (Figure 1A), and its expression was also remarkably lower in the 5 BC cell lines – MCF-7, MDA-MB-231, MDA-MB-435, T47D, and SKBR-3 – than in the normal human mammary epithelial cell line MCF-10A (Figure 1B). The correlation between the expression of lncRNA TFAP2A-AS1 and the clinicopathological features in breast cancer tissues is shown in Table 1. In addition, we analyzed the overall survival rate of BC patients with low or high TFAP2A-AS1 expression. Results indicated that the 20 patients with low TFAP2A-AS1 expression had worse prognosis than the 10 patients with high TFAP2A-AS1 expression (Figure 1C, 1D).

Overexpression of TFAP2A-AS1 significantly inhibited the progression of BC *in vitro* and *in vivo*

To assess the cellular distribution of TFAP2A-AS1 in BC cells, we examined the cellular location of TFAP2A-AS1 in MCF-7 and MDA-MB-231 cells. Results showed that TFAP2A-AS1 resided in both nucleus and cytoplasm of MCF-7 and MDA-MB-231 cells; however, the majority of TFAP2A resided in the

Indexed in: [Current Contents/Clinical Medicine] [SCI Expanded] [ISI Alerting System] [ISI Journals Master List] [Index Medicus/MEDLINE] [EMBASE/Excerpta Medica] [Chemical Abstracts/CAS]

Table 2. MicroRNAs that predicted sponge by TFAP2A-AS1.

Motif Name	Position	Length	Minimum free energy	Score
hsa-miR-25-5p	581~600	20	–23.28	161
hsa-miR-99b-3p	78~99	22	–20.6	161
hsa-miR-484	249~275	27	–29.6	161
hsa-miR-490-3p	953~977	25	–24.09	164
hsa-miR-518c-5p	664~686	23	–25.25	164
hsa-miR-516b-5p	663~685	23	–20.35	165
hsa-miR-625-5p	953~972	20	–27.25	166
hsa-miR-933	29~55	27	–31.71	164
hsa-miR-1247-5p	161~186	26	–32.34	163
hsa-miR-3131	300~324	25	–28.28	168
hsa-miR-3148	865~888	24	–20.48	167
hsa-miR-4269	1233~1253	21	–26.25	163
hsa-miR-3612	671~694	24	–28.53	162
hsa-miR-4430	550~567	18	–25.51	162
hsa-miR-4465	1054~1075	22	–23.92	168
hsa-miR-4687-3p	416~438	23	–28.32	169
hsa-miR-4723-3p	14~37	24	–34.84	169
hsa-miR-4763-3p	589~613	25	–31.7	165

cytoplasm (Figure 2A, 2B). We then established a TFAP2A-AS1-overexpressed cell model in MCF-7 and MDA-MB-231 cells by transfecting them with TFAP2A-AS1. qRT-PCR results indicated that the TFAP2A-AS1 expression in MCF-7 and MDA-MB-231 cells transfected with TFAP2A-AS1 were significantly higher than those cells transfected with TFAP2A-AS1 negative control (Figure 2C, 2D). Subsequently, a series of functional assays were performed in the TFAP2A-AS1-overexpressed cell models to detect the effects of TFAP2A-AS1 on cell cycle, apoptosis, viability, and invasion. Results from flow cytometry analysis showed that TFAP2A-AS1 overexpression significantly reduced the numbers of MCF-7 and MDA-MB-231 cells in S phase (Figure 2E–2H). Western blot assay showed a significant downregulation of CDK6, cyclin D1, and cyclin E1 in TFAP2A-AS1-overexpressed MCF-7 and MDA-MB-231 cells compared to the control group (Figure 2I, 2J). Apoptosis analysis indicated a marked upregulation of apoptosis rate in TFAP2A-AS1-overexpressed MCF-7 and MDA-MB-231 cells compared to the control group (Figure 2K, 2L). CCK-8 assay showed a significant suppression of cell viability in TFAP2A-AS1-transfected MCF-7 and MDA-MB-231 cells (Figure 3A, 3B). Transwell assay showed a remarkable decrease of invasive cell numbers in MCF-7 and MDA-MB-231 cells transfected with TFAP2A-AS1 compared with the control groups (Figure 3C, 3D). To further explore the effects of TFAP2A-AS1 *in vivo*, TFAP2A-AS1-overexpressed and control MCF-7 cells were injected subcutaneously into nude mice. Compared with control xenografts, the tumor volume and weight were significantly smaller in the TFAP2A-AS1-overexpressed group (Figure 3E, 3F).

TFAP2A-AS1 acted as a competing endogenous RNAs (ceRNAs) in BC by sponging miR-933

Through bioinformatics analysis, the potential binding sites of miR-933 in TFAP2A-AS1 were predicted (Table 2, Figure 4A) and the secondary structure of miR-933/TFAP2A-AS1 match was shown (Figure 4B). Dual-luciferase reporter assay was used to verify the interaction between TFAP2A and miR-933 in MCF-7 cells. Results showed that miR-933 mimics remarkably attenuated the luciferase activity of the wild-type reporter of TFAP2A-AS1; however, miR-933 mimics failed to influence the luciferase activity of mutant reporter of TFAP2A in MCF-7 cells (Figure 4C). RNA RIP and pull-down assays were carried out in MCF-7 cells to further verified the interaction between TFAP2A-AS1 and miR-933. Results from RNA RIP showed that TFAP2A-AS1 and miR-933 bind directly to Ago2 (Figure 4D). RNA pull-down assay indicated a specific enrichment of TFAP2A-AS1 in the biotin-labeled wild-type miR-933 group (Figure 4E). Furthermore, TFAP2A-AS1-overexpressed MCF-7 and MDA-MB-231 cells showed a significant

Indexed in: [Current Contents/Clinical Medicine] [SCI Expanded] [ISI Alerting System] [ISI Journals Master List] [Index Medicus/MEDLINE] [EMBASE/Excerpta Medica] [Chemical Abstracts/CAS]

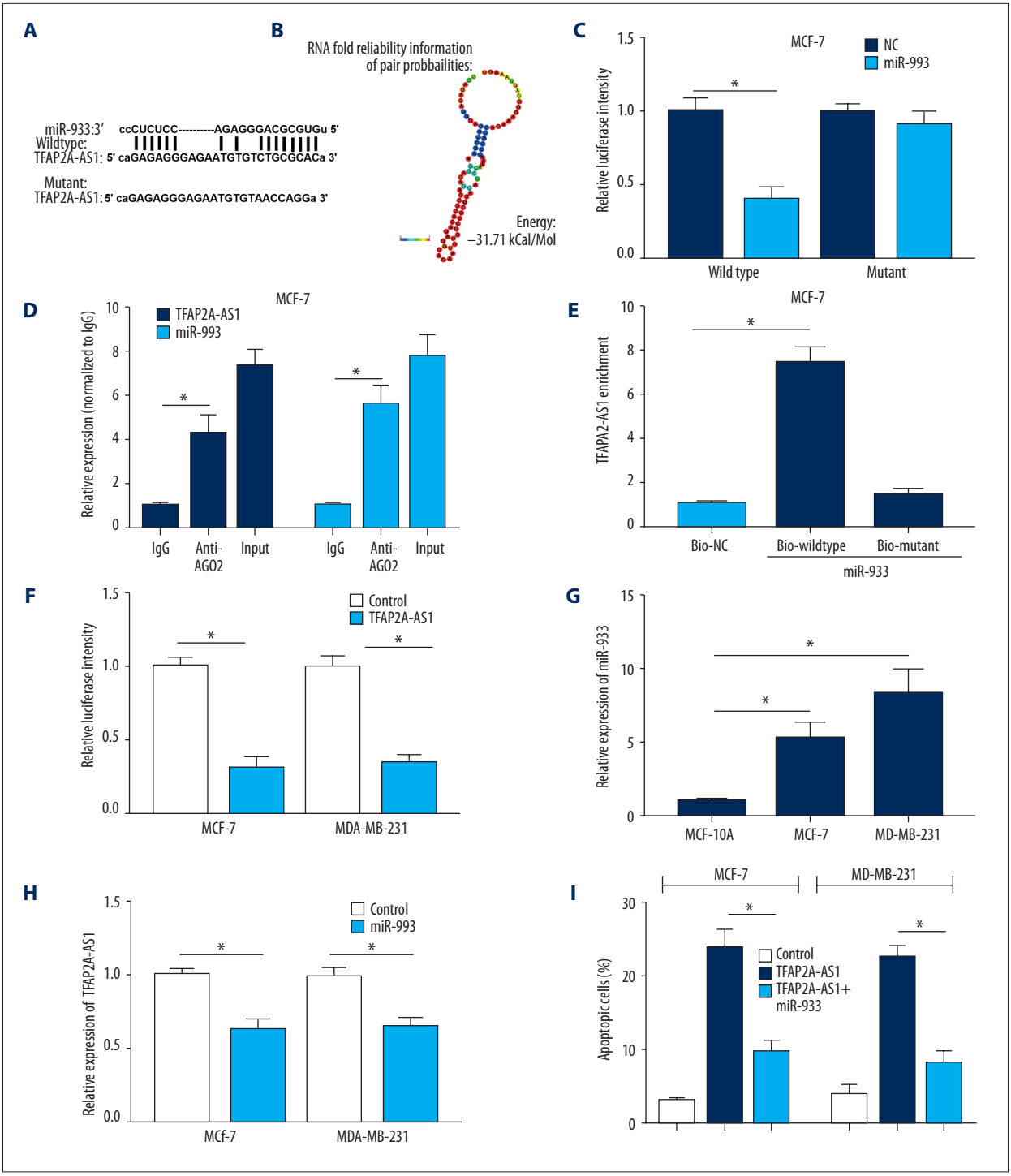

Figure 4. Interaction between TFAP2A-AS1 and miR-933 in BC cells. (**A**) The putative binding site of miR-933 in TFAP2A-AS1. (**B**) RNA secondary structure of TFAP2A-AS1 was predicted using the Vienna RNA fold server. (**C**) Dual-luciferase reporter assay was carried out to evaluate the interaction of TFAP2A-AS1 and miR-933. (**D**) RNA RIP experiments were performed in MCF-7 cells and the co-precipitated RNA was analyzed by qRT-PCR. (**E**) RNA pull-down assay followed by qRT-PCR were performed to assess the interaction between TFAP2A-AS1 and miR-933 using biotin-labeled miR-933. (**F**) Relative mRNA expression of miR-933 was measured in TFAP2A-AS1 treated MCF-7 and MDA-MB-231 cells. (**G**) Relative mRNA expression of miR-933 was detected in MCF-10A, MCF-7 and MDA-MB-231 cells using qRT-PCR. (**H**) Relative mRNA expression of TFAP2A-AS1 in miR-933 transfected MCF-7 and MDA-MB-231 cells were examined by qRT-PCR. (**I**) Cell apoptosis of MCF-7 and MDA-MB-231 cells transfected with control or TFAP2A-AS1 or co-transfected with TFAP2A-AS1 and miR-933 were evaluated by flow cytometry.

Indexed in: [Current Contents/Clinical Medicine] [SCI Expanded] [ISI Alerting System] [ISI Journals Master List] [Index Medicus/MEDLINE] [EMBASE/Excerpta Medica] [Chemical Abstracts/CAS]

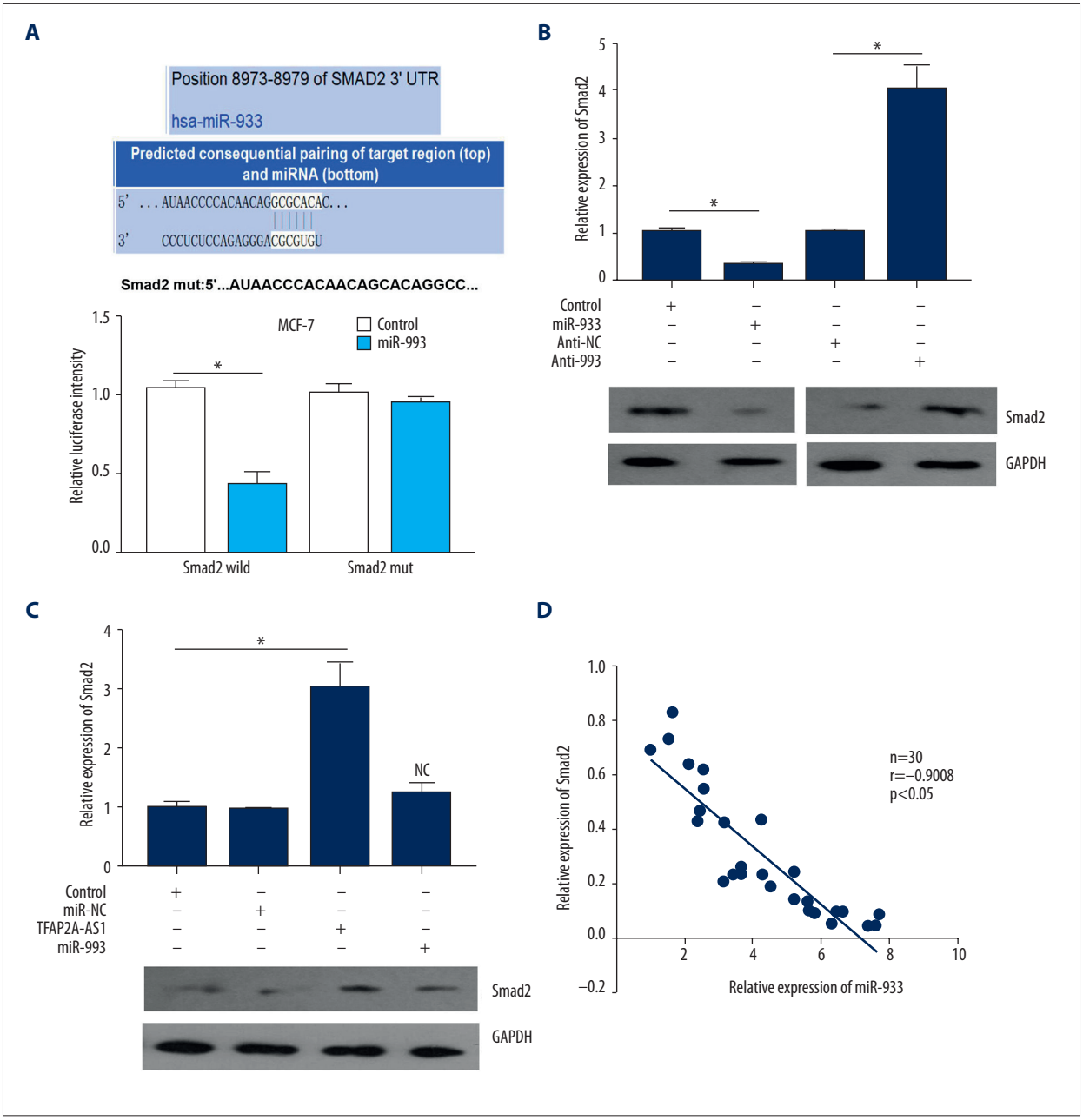

Figure 5. Interaction between miR-933 and SMAD2 in BC cells. (**A**) **Upper panel:** the putative binding site of miR-933 in the 3'-UTR of SMAD2. **Lower panel:** the interaction between miR-933 and SMAD2 was verified by dual-luciferase reporter assay. (**B**) Relative protein expression of Smad2 was determined by Western blot assay in MCF-7 cells transfected with miR-933 mimics or inhibitor (anti-933). (**C**) Relative protein expression of Smad2 was measured in TFAP2A-AS1- and miR-93 treated MCF-7 cells by Western blot assay. (**D**) Correlation between miR-933 and Smad2 expression in MCF-7 cells was evaluated

downregulation of miR-933 (Figure 4F). The miR-933 expression in MCF-7 and MDA-MB-231 cells was significantly higher than in MCF-10A cells (Figure 4G), and TFAP2A-AS1 expression was significantly reduced in the MCF-7 and MDA-MB-231 cells transfected with miR-933 mimics compared to the control cells (Figure 4H). Apoptosis analysis indicated a marked rescue of apoptosis rate in TFAP2A-AS1 and miR-933 co-transfection BC cells, which further supports that TFAP2A-AS1 acts as a competing endogenous RNA (ceRNA) in BC by sponging miR-933 (Figure 4I).

SMAD2 was directly targeted gene of miR-933

By using bioinformatics tools, we revealed that there was a binding site of miR-933 in the 3'-UTR of SMAD2 (Figure 5A,

Indexed in: [Current Contents/Clinical Medicine] [SCI Expanded] [ISI Alerting System] [ISI Journals Master List] [Index Medicus/MEDLINE] [EMBASE/Excerpta Medica] [Chemical Abstracts/CAS]

upper panel). Subsequently, to further validate the interaction between miR-933 and TFAP2A-AS1 in BC cells, the wild-type 3'-UTR of SMAD2 containing the putative miR-933 binding site or its mutant type were cloned into the luciferase reporter plasmid. Results from dual-luciferase reporter assay showed that miR-933 mimics obviously attenuated the luciferase intensity driven by the wild-type SMAD2; however, the luciferase intensity driven by the mutant SMAD2 was not affected by miR-933 in MCF-7 cells (Figure 5A, lower panel). Western blot assay was used to detect the protein expression of SMAD2 in MCF-7 cells transfected with miR-933 mimics or inhibitor (anti-933), showing that SMAD2 expression was significantly downregulated in the miR-933-treated group compared to control cells, and SMAD2 expression was remarkably upregulated in the anti-933 treated group compared with the anti-NC treated group (Figure 5B). Furthermore, the protein expression of SMAD2 in TFAP2A-AS1-overexpressed MCF-7 cells was significantly upregulated, and this TFAP2A-AS1 induced upregulation of SMAD2 was reversed by miR-933 (Figure 5C). In addition, results from Spearman's correlation analysis showed a significant negative correlation between SMAD2 and miR-933 expression in BC tissues (Figure 5D).

Discussion

BC poses a serious threat to the health of women worldwide, and it currently is the leading cause of death in women [17]. Thus, BC prevention and therapy are important topics in modern medical research [18]. Although the exact molecular mechanisms of the tumorigenesis of BC remain largely unknown, increasing evidence suggests that lncRNAs contribute to BC pathogenesis [19,20]. With the rapid development of related research, more and more lncRNAs expression profiles are demonstrated to be involved in the pathogenic progress of BC [21]. For example, lncRNA-LIN01296 was revealed to be upregulated in BC tissues and cell lines, and its upregulation was demonstrated to be associated with larger tumor size and advanced clinical TNM stage; moreover, knockdown of LINC01296 inhibited BC cell growth *in vitro* and *in vivo* [22]. TFAP2A-AS1 is a newly discovered lncRNA located at chromosome 6q24.3, with undetermined biological functions. In this study, qRT-PCR showed that TFAP2A-AS1 expression was significantly downregulated in BC, and BC patients with low TFAP2A-AS1 exhibited a worse prognosis. In the functional assays, we found that overexpression significantly suppressed tumor growth *in vitro* and *in vivo*.

It is well documented that lncRNAs exhibit multiple biological functions in tumor cells by serving as miRNAs sponges to indirectly regulate the expression of targeted genes [16,23–25]. Therefore, to determine the mechanisms underlying the effects of TFAP2A-AS1 on BC, bioinformatics analysis was performed to screen the targeted miRNAs of TFAP2A-AS1. Following validation by dual-luciferase reporter and RNA RIP assays, TFAP2A-AS1 was demonstrated to sponge miR-933 in BC cells.

We further explored whether TFAP2A-AS1 exhibited its tumor-suppressive effects by sponging miR-933 to indirectly regulate the expression of targeted genes. We predicted and verified the targeted genes of miR-933 by bioinformatics tools and dual-luciferase reporter assay, respectively, showing that the 3'-UTR of SMAD2 showed bindings sites for miR-933. The transforming growth factor-β (TGF-β) signaling pathway was well documented to play important functions in cell proliferation, apoptosis, differentiation, and embryonic development [26,27], and the SMAD family was demonstrated to transduce the signals form TGF- β signaling pathway to participate the biological processes by activating receptor serine/threonine kinases [28,29]. The proteins of the SMAD family all have 1 conserved N-terminal Mad homology domain-1 (MH1) and 1 C-terminal Mad homology domain-2 (MH2) [29,30]. Activation of the TGF- β/SMAD signaling pathway was reported to promote tumor progression in multiple human cancers, including lung cancer, breast cancer, and renal cell cancer [31–33]. In the present study, overexpression of TFAP2A-AS1 upregulated the expression of SMAD2, whereas miR-933 reversed this upregulation of SMAD2 induced by TFAP2A-AS1. In addition, there was a negative correlation between miR-933 and SMAD2 in BC.

Conclusions

The most important results of the present study are: 1) lncRNA TFAP2A-AS1 was significantly downregulated in BC tissues and cell lines; 2) Silencing of TFAP2A-AS1 suppressed the tumorigenesis of BC; and 3) mechanistic analysis showed that TFAP2A-AS1 regulated SMAD2 by specifically sponging miR-933. Our study discloses a novel TFAP2A-AS1-miR-933-SMAD2 signaling pathway involved in BC cell progression. Therefore, TFAP2A-AS1 may serve as a therapeutic target for BC treatment.

conflict of interest

None.

Indexed in: [Current Contents/Clinical Medicine] [SCI Expanded] [ISI Alerting System] [ISI Journals Master List] [Index Medicus/MEDLINE] [EMBASE/Excerpta Medica] [Chemical Abstracts/CAS]

References:

1. Thrift-Perry M, Cabanes A, Cardoso F et al: Global analysis of metastatic breast cancer policy gaps and advocacy efforts across the patient journey. Breast, 2018; 41: 93–106
2. Crabtree JS, Miele L: Breast cancer stem cells. Biomedicines, 2018; 6(3): pii: E77
3. Cedolini C, Bertozzi S, Londero AP et al: Type of breast cancer diagnosis, screening, and survival. Clin Breast Cancer, 2014; 14(4): 235–40
4. Anothaisintawee T, Wiratkapun C, Lerdsitthichai P et al: Risk factors of breast cancer: A systematic review and meta-analysis. Asia Pac J Public Health, 2013; 25(5): 368–87
5. Turkoz FP, Solak M, Petekkaya I et al: Association between common risk factors and molecular subtypes in breast cancer patients. Breast, 2013; 22(3): 344–50
6. Albuquerque RC, Baltar VT, Marchioni DM: Breast cancer and dietary patterns: A systematic review. Nutr Rev, 2014; 72(1): 1–17
7. Peart O: Breast intervention and breast cancer treatment options. Radiol Technol, 2015; 86(5): 535M–58M; quiz 559–62
8. Guo L, Zhao Y, Yang S et al: An integrated analysis of miRNA, lncRNA, and mRNA expression profiles. Biomed Res Int, 2014; 2014: 345605
9. Anastasiadou E, Faggioni A, Trivedi P, Slack FJ: The Nefarious nexus of noncoding RNAs in cancer. Int J Mol Sci, 2018; 19(7): pii: E2072
10. Lekka E, Hall J: Noncoding RNAs in disease. FEBS Lett, 2018; 592(17): 2884–900
11. Dang Y, Wei X, Xue L et al: Long non-coding RNA in glioma: Target miRNA and signaling pathways. Clin Lab, 2018; 64(6): 887–94
12. Wang L, Liu J: [Research progress of competing endogenous RNA]. Sheng Wu Yi Xue Gong Cheng Xue Za Zhi, 2017; 34(6): 967–71 [in Chinese]
13. Bayoumi AS, Sayed A, Broskova Z et al: Crosstalk between long noncoding RNAs and microRNAs in health and disease. Int J Mol Sci, 2016; 17(3): 356
14. Thomson DW, Dinger ME: Endogenous microRNA sponges: Evidence and controversy. Nat Rev Genet, 2016; 17(5): 272–83
15. King VM, Borchert GM: MicroRNA expression: Protein participants in microRNA regulation. Methods Mol Biol, 2017; 1617: 27–37
16. Liu H, Li H, Jin L et al: Long noncoding RNA GAS5 suppresses 3T3-L1 cells adipogenesis through miR-21a-5p/PTEN signal pathway. DNA Cell Biol, 2018; 37(9): 767–77
17. Loibl S, Denkert C, von Minckwitz G: Neoadjuvant treatment of breast cancer – Clinical and research perspective. Breast, 2015; 24(Suppl. 2): S73–77
18. Bai X, Ni J, Beretov J, Graham P, Li Y: Cancer stem cell in breast cancer therapeutic resistance. Cancer Treat Rev, 2018; 69: 152–63
19. Gu J, Wang Y, Wang X et al: Effect of the lncRNA GAS5-MiR-23a-ATG3 axis in regulating autophagy in patients with breast cancer. Cell Physiol Biochem, 2018; 48(1): 194–207
20. Chang L, Hu Z, Zhou Z, Zhang H: Linc00518 contributes to multidrug resistance through regulating the MiR-199a/MRP1 axis in breast cancer. Cell Physiol Biochem, 2018; 48(1): 16–28
21. Tian T, Gong Z, Wang M et al: Identification of long non-coding RNA signatures in triple-negative breast cancer. Cancer Cell Int, 2018; 18: 103
22. Jiang M, Xiao Y, Liu D et al: Overexpression of long noncoding RNA LINC01296 indicates an unfavorable prognosis and promotes tumorigenesis in breast cancer. Gene, 2018; 675: 217–24
23. Song X, Shan D, Chen J, Jing Q: miRNAs and lncRNAs in vascular injury and remodeling. Sci China Life Sci, 2014; 57(8): 826–35
24. Li W, Jia G, Qu Y et al: Long non-coding RNA (lncRNA) HOXA11-AS promotes breast cancer invasion and metastasis by regulating epithelial-mesenchymal transition. Med Sci Monit, 2017; 23: 3393–403
25. Wu C, Luo J: Long non-coding RNA (lncRNA) urothelial carcinoma-associated 1 (UCA1) enhances tamoxifen resistance in breast cancer cells via inhibiting mTOR signaling pathway. Med Sci Monit, 2016; 22: 3860–67
26. Hu HH, Chen DQ, Wang YN et al: New insights into TGF-beta/Smad signaling in tissue fibrosis. Chem Biol Interact, 2018; 292: 76–83
27. Furler RL, Nixon DF, Brantner CA et al: TGF-beta sustains tumor progression through biochemical and mechanical signal transduction. Cancers (Basel), 2018; 10(6): pii: E199
28. Chen L, Yang T, Lu DW et al: Central role of dysregulation of TGF-beta/Smad in CKD progression and potential targets of its treatment. Biomed Pharmacother, 2018; 101: 670–81
29. Witkowska M, Smolewski P: [SMAD family proteins: the current knowledge on their expression and potential role in neoplastic diseases]. Postepy Hig Med Dosw (Online), 2014; 68: 301–9 [in Polish]
30. Chai N, Li WX, Wang J et al: Structural basis for the Smad5 MH1 domain to recognize different DNA sequences. Nucleic Acids Res, 2015; 43(18): 9051–64
31. Kaur G, Li CG, Chantry A et al: SMAD proteins directly suppress PAX2 transcription downstream of transforming growth factor-beta 1 (TGF-beta1) signalling in renal cell carcinoma. Oncotarget, 2018; 9(42): 26852–67
32. Deng G, Chen L, Zhang Y et al: Fucosyltransferase 2 induced Epithelial-mesenchymal transition via TGF-beta/Smad signaling pathway in lung adenocarcinaoma. Exp Cell Res, 2018; 370(2): 613–22
33. Gonzalez-Gonzalez A, Munoz-Muela E, Marchal JA et al: Activating transcription factor 4 modulates TGFbeta-induced aggressiveness in triple negative breast cancer via SMAD2/3/4 and mTORC2 signaling. Clin Cancer Res, 2018 [Epub ahead of print]

Indexed in: [Current Contents/Clinical Medicine] [SCI Expanded] [ISI Alerting System] [ISI Journals Master List] [Index Medicus/MEDLINE] [EMBASE/Excerpta Medica] [Chemical Abstracts/CAS]